



# Nontrivial Relations Among Particle Collision, Relative Motion and Clustering in Turbulent Clouds: Computational Observation and Theory.

Ewe-Wei Saw<sup>1,2</sup> and Xiaohui Meng<sup>1</sup>

<sup>1</sup>School of Atmospheric Sciences and Guangdong Province Key Laboratory for Climate Change and Natural Disaster Studies, Sun Yat-Sen University, Zhuhai, China

<sup>2</sup>Ministry of Education Key Laboratory of Tropical Atmosphere-Ocean System, Zhuhai, China

**Correspondence:** E.-W. Saw (ewsaw3@gmail.com), X. Meng (mengxh7@mail2.sysu.edu.cn)

## Abstract.

Considering turbulent clouds containing small heavy particles, we investigate the reverse effect of particle collision, in particular collision-&-coagulation, on particle clustering and relative motion. We perform various cases of direct numerical simulation (DNS) of coagulating particles in isotropic turbulent flow and find that, due to collision-coagulation, the radial distribution functions (RDF) fall-off dramatically at scales  $r \sim d$  (where  $d$  is the particle diameter) to small but finite values; while the mean radial-component of particle relative velocities (MRV) increase sharply in magnitudes. Based on a previously proposed Fokker-Planck (drift-diffusion) framework, we derive a theoretical account of the relationship among particle collision-coagulation rate, RDF and MRV. The theory includes contribution from turbulent-fluctuations absent in earlier mean-field theories. We show numerically that the theory accurately account for the DNS results. We also proposed a phenomenological model for the MRV which is accurate when calibrated using 4th moments of the fluid velocities. We uncover a paradox: the unjustified accuracy of the differential version of the theory. Our result demonstrate strong coupling between RDF and MRV and implies that earlier isolated studies on either RDF or MRV have limited relevance for predicting particle collision rate.

## 1 Introduction

The motion and interactions of small particles in turbulence has fundamental implications for atmospheric clouds, specifically, it is relevant to the time-scale of rain formation particularly in warm-clouds (Falkovich et al., 2002; Wilkinson et al., 2006; Grabowski and Wang, 2013) [a similar problem also applies to planet formation in astrophysics (Johansen et al., 2007)]. It is also important for engineers who are designing future, greener, combustion engines, as this is a scenario they wish to understand and control in order to increase fuel-efficiency (Karnik and Shrimpton, 2012). Cloud particles or droplets, due to their inertia, are known to be ejected from turbulent vortices and thus form clusters (Wood et al., 2005; Bec et al., 2007; Saw et al., 2008; Karpińska et al., 2019) i.e. regions of enhanced particle-density; this together with collision of droplets is of direct relevance for the mentioned applications. Due to the technical difficulty of obtaining extensive and systematic experimental or field data on particle/droplet collision in turbulent cloud, many of the recent studies rely on direct numerical simulation (DNS), example of



which could be found in e.g. (Onishi and Seifert, 2016; Wang et al., 2008) and reference therein. Up until now, we do not have definitive answers to basic questions such as how to calculate particle collision rate from basic turbulence-particle parameters and what is the exact relation between collision and particle clustering and/or motions, for, as we shall see, our work reveals that collision-coagulation causes profound changes in both mean radial-component of relative particle velocity (MRV) and radial distribution function (RDF), questioning earlier understanding of the problem (RDF is a metric of the degree of particle clustering). The difficulty of this problem is in part related to the fact that turbulence is, even by itself, virtually intractable theoretically due to its nonlinear and complex nature.

The quest for a theory of particle collision in turbulence started in 1956, when Saffman and Turner (1956) derived a mean-field formula for collision rate of finite size, inertialess, particles. In another landmark work (Sundaram and Collins, 1997), a general relation among collision-rate ( $R_c$ ), particle clustering and mean particle relative radial velocity was presented:  $R_c/(n_1 n_2 V) = 4\pi d^2 g(d) \langle w_r(d) | w_r \leq 0 \rangle_*$ , where  $g(r)$  is the RDF,  $w_r$  is the radial component of relative velocity between two particles,  $\langle w_r(d) | w_r \leq 0 \rangle_*$  is the MRV i.e. a (conditional) mean of  $w_r$  (averaged over all particle pairs);  $n_i$ 's are global averages of particle number density,  $V$  is the spatial volume of the domain,  $d$  the particle diameter. The remarkable simplicity of this finding inspired a "separation paradigm", which is the idea that one could study the RDF or MRV separately (which are technically easier), the independent results from the dual may be combined to accurately predicts  $R_c$  (an idea that we subsequently challenge). Another work of special interest here is the drift-diffusion model by Chun, Koch et al. (Chun et al., 2005) (hereafter: CK theory) (note: there are other equivalent theories (Balkovsky et al., 2001; Zaichik and Alipchenkov, 2003)). The CK theory, derived for non-colliding particles in the limit of vanishing particle Stokes number  $St$  (a quantity that reflects the importance of the particle's inertia in dictating its motion in turbulence), correctly predicted the power-law form of the RDF (Reade and Collins, 2000; Saw et al., 2008) and have seen remarkable successes over the years including the accurate account of the modified RDF of particles interacting electrically (Lu et al., 2010) and hydrodynamically (Yavuz et al., 2018).

Here, we first present results on RDF and MRV for particle undergoing collision-coagulation<sup>1</sup>. The data is obtained via direct numerical simulation (DNS), which is the gold-standard computational method in term of accuracy and completeness for solving the most challenging fluid dynamics problem i.e. turbulent flows. DNS solves the fundamental equation of fluid dynamics, the Navier-Stokes Equation, with full resolution and without turbulence modeling. The accuracy of DNS for various turbulent-flows have been experimentally validated for decades (see e.g. the compilation of results in Pope (2000)); while for simulating dynamics of small heavy particles, experimental validation of its accuracy could be found in Salazar et al. (2008); Saw et al. (2012b, 2014); Dou et al. (2018).

Analysis of the DNS results is then followed by a theoretical account of the relations between collision-rate, RDF and MRV that includes mean-field contributions (Saffman and Turner, 1956; Sundaram and Collins, 1997) and contributions from turbulent fluctuations (absent from earlier theories (Saffman and Turner, 1956; Sundaram and Collins, 1997)). The theory is derived from the Fokker-Planck (drift-diffusion) framework first introduced in the CK theory (Chun et al., 2005). We shall see

<sup>1</sup>Coagulation is, in a sense, the simplest outcome of collision. In the sequel we shall argue that the major qualitative conclusions of our work also applies to cases with other collisional outcome.



55 that the main effect of collision-coagulation is the enhanced asymmetry in the particle relative velocity distribution<sup>2</sup> and that this leads to nontrivial outcomes.

## 2 Direct Numerical Simulation (DNS)

To observe how particle collision-coagulation affects RDF and MRV, we performed direct numerical simulation (DNS) of steady-state isotropic turbulence embedded with particles of finite but sub-Kolmogorov size. We solve the incompressible Navier-Stokes Equations (Eq. (1)) using the standard pseudo-spectral method (Rogallo, 1981; Pope, 2000; Mortensen and Langtangen, 2016) inside a triply periodic cubic-box.

$$\frac{\partial \mathbf{u}}{\partial t} + \mathbf{u} \cdot \nabla \mathbf{u} = -\frac{1}{\rho} \nabla p + \nu \nabla^2 \mathbf{u} + \mathbf{f}(\mathbf{x}, \mathbf{t}),$$
$$\nabla \cdot \mathbf{u} = 0, \quad (1)$$

65 where  $\rho, p, \nu, \mathbf{f}$  are the fluid density, pressure, kinematic viscosity, imposed forcing respectively. The velocity field is discretized on a  $256^3$  grid. Aliasing resulting from Fourier transform of truncated series is removed via a 2/3-dealiasing rule (Rogallo, 1981). A statistically stationary and isotropic turbulent flow is achieved by continuously applying random forcing to the lowest wave-numbers until the flow's energy spectrum is in steady-state. The 2nd-order Runge-Kutta time stepping was employed. Further details of such a standard turbulence simulator can be found in e.g. (Pope, 2000; Rogallo, 1981; Mortensen and Langtangen, 2016).

Particles in the simulations are advected via a viscous Stokes drag force:

$$d\mathbf{v}/dt = (\mathbf{u} - \mathbf{v})/\tau_p,$$

where  $\mathbf{u}, \mathbf{v}$  are the local fluid and particle velocity respectively,  $\tau_p$  is the particle inertia response time. The focus of our study is on the effect of particle collision-coagulation in the simplest fluid dynamic setting so that its implication and fundamental interaction with turbulence can be fully understood before moving on to more complex settings in future works. For this reason, we choose not to include hydrodynamic interactions and gravitational settling in the dynamic of the particles (this implies that if practical applicability is of concern, the current results only applies to cloud particles with gravitational terminal velocities that are small compared to the velocity scale of the smallest turbulent eddies, e.g. particle of size  $\lesssim 50 \mu m$  in atmospheric clouds). In this context, the particle Stokes number, defined as  $\tau_p/\tau_\eta$  where  $\tau_\eta$  is the Kolmogorov time-scale, could be expressed as  $St = \frac{1}{18}(\rho_p/\rho)(d/\eta)^2$ , where  $\rho_p/\rho$  is the particle-to-fluid mass-density ratio,  $d$  is the particle diameter,  $\eta$  the Kolmogorov length-scale. Time-stepping of the particle motion is done using a 2nd-order modified Runge-Kutta method with "exponential integrator" that is accurate even for  $\tau_p$  much smaller than the fluid's time-step (Ireland et al., 2013). The particles are spherical and collide when their volumes overlap and a new particle is formed conserving volume and momentum. We continuously, randomly, inject new particles into the flow so that the system is in a steady-state after some time. Statistical analysis is done at steady-state on monodisperse particles (involving particles with the same  $St$ ).

<sup>2</sup>In the collision-less case, the asymmetry is much weaker and is related to viscous dissipation of energy in turbulence Pope (2000).



$Re_\lambda$	$\nu [10^{-2}m^2/s]$	$u_{rms} [dm/s]$	$\epsilon [10^{-2}m^2/s^3]$	$\eta [dm]$	$\tau_\eta [s]$	$L_c [dm]$	$d [dm]$
133	0.001	0.613	0.117	0.00962	0.0925	$2\pi$	$d_*$ or $2d_*$

**Table 1.** Values of the parameters in the DNS. (Note:  $dm$  = decimeter). Respectively, we have the Taylor-scale Reynolds number, kinematic viscosity of the fluid, root-mean-square of fluid velocity, kinetic energy dissipation rate, Kolmogorov length- and time-scale, length of the simulation cube and particle diameters considered. We have introduced  $d_*$  to represent the specific value:  $9.49 \times 10^{-4}$  (explanation is given later in the text). We have chosen the units of the length (time) scale in the DNS to be in decimeter (second), such that  $\nu$  is nearly its typical value in the atmosphere.

The values of key parameters of the DNS are given in Table 1.

### 3 Basics of the Drift-Diffusion Theory

As described in (Chun et al., 2005), in the limit of  $St \ll 1$ , particle motions are closely tied to the fluid's and, to leading order, completely specified by the particle position and the fluid's velocity gradients. Now consider the fundamental Fokker-Planck equation which is closed and deterministic (see e.g. Appendix J in (Pope, 2000)):

$$\frac{\partial P}{\partial t} + \frac{\partial(W_i P)}{\partial r_i} = 0, \quad (2)$$

where  $P \equiv P(r_i, t | \Gamma_{ij}(t))$  is the (per volume) probability density (PDF) for a secondary particle (which could have any history) to be at vector position  $r_i$  relative to a primary particle at time  $t$ , conditioned on a fixed and known history of the velocity gradient tensor along the primary particle's trajectory  $\Gamma_{ij}(t)$ ,  $W_i$  is the mean velocity of secondary particles relative to the primary, under the same condition. Note:  $W_i$  is a conditional-average, while  $w_i$  denotes a realization of relative velocity between two particle.

From this, one could derive an equation for  $\langle P \rangle(r)$  (where  $\langle \cdot \rangle$  implies ensemble averaging over primary particle histories):

$$\frac{\partial \langle P \rangle}{\partial t} + \frac{\partial}{\partial r_i} (\langle W_i \rangle \langle P \rangle + \langle W_i P' \rangle) = 0. \quad (3)$$

However, this equation is not closed due to correlation between the fluctuating terms  $W_i$  and  $P' \equiv P - \langle P \rangle$ . The correlation  $\langle W_i P' \rangle$  can be written in terms of a drift flux and diffusive flux (detailed derivation is well described in (Chun et al., 2005)), such that we have:

$$\frac{\partial \langle P \rangle}{\partial t} + \frac{\partial}{\partial r_i} (q_i^d + q_i^D) + \frac{\partial (\langle W_i \rangle \langle P \rangle)}{\partial r_i} = 0, \quad (4)$$

where the drift flux is:

$$q_i^d = - \int_{-\infty}^t \left\langle W_i(\mathbf{r}, t) \frac{\partial W_l}{\partial r'_l}(\mathbf{r}', t') \right\rangle \langle P \rangle(\mathbf{r}', t') dt',$$



and the diffusive flux is:

$$q_i^D = - \int_{-\infty}^t \langle W_i(\mathbf{r}, t) W_j(\mathbf{r}', t') \rangle \frac{\partial \langle P \rangle}{\partial r'_j}(\mathbf{r}', t') dt',$$

where  $\mathbf{r}'$  satisfies a characteristic equation:  $\frac{\partial r'_i}{\partial t'} = W_i(\mathbf{r}', t')$ , with boundary condition: when  $t' = t$ ,  $r'_i = r_i$ .

#### 4 DNS Results, Theory and Discussion

110 We compute the RDF via  $g(r) = N_{pp}(r) / [\frac{1}{2} N(N-1) \delta V_r / V]$ , where  $N_{pp}(r)$  is the number of particle pairs found to be separated by distance  $r$ ,  $\delta V_r$  is the volume of a spherical shell of radius  $r$  and infinitesimal thickness  $\delta r$ ,

Figure 1 shows the RDFs obtained for particles of different Stokes numbers and sizes. The cases shown includes  $St = 0.22, 0.54$  in panel-a, and  $St = 0.054, 0.001$  in panel-b. In all cases, except one, the particles are of the same size  $d = d_*$ , where  $d_*$  represents the specific value of  $d_* = 9.49 \times 10^{-4} dm$ , chosen so that the particle sizes are one order of magnitude  
115 smaller than the Kolmogorov scale ( $\eta$ ), thus allowing us to still observe a regime ( $3d \lesssim r \lesssim 30\eta$ ) of power-law RDFs. To shows the effect of changing particle size, panel-a also includes a case of ( $St = 0.54, d = 2d_*$ ) for comparison. The main figure in panel-a shows clearly that the RDFs for these colliding-coagulating particles fall-off dramatically at  $r \sim d$ , in contrast to what was seen in earlier studies of non-colliding particles where  $g(r)$  are simple power-laws (Chun et al., 2005; Saw et al., 2008). We see that as  $r$  approaches  $d$  the steepness of the curve (see e.g. the blue-circles) increases as  $g(r)$  drops-off, this  
120 and the fact that the abscissa is logarithmic implies that  $\frac{\partial g}{\partial r}$  is increasing exponentially in the process. As a consequence, it is difficult to discern from these plots if the limit of  $g(r)$  are still nonzero at particle contact ( $r \rightarrow d$ ), which is a important question as  $\lim_{r \rightarrow d} \{g(r)\} = 0$  implies that the mean-field formula of Sundaram and Collins (1997) has zero contribution towards  $R_c$ , i.e. collision rate is fully due to turbulent-fluctuations. It is only by re-plotting  $g(r)$  versus  $r-d$  (see insets in Fig. 1), and using a remarkable resolution that is  $10^3$  finer than  $d$ , that we see a convincing trend supporting a finite  $g(r \rightarrow d)$ .

125 The strong effect of particle collision on the RDF (also on MRV as we shall we later) challenges the validity of the "separation paradigm". Also clear in panel-a is the observation that with changing particle-size ( $d$ ) the location of the sharp fall-off merely shifts to where the new value of  $d$  is. We note that similar fall-off of RDF was previously observed (Sundaram and Collins, 1997) but a complete analysis and theoretical understanding was lacking. Also, a study on multiple collisions (Voßkuhle et al., 2013) had hinted at the potential problem with the separation paradigm.

130 Another observation is that in the power-law regime ( $3d \lesssim r \lesssim 30\eta$ ), the RDFs appear (as expected) as straight-lines with slopes (i.e. power-law exponents) that increase with  $St$  and are numerically consistent with those found for non-colliding particles (see e.g. (Saw et al., 2012b)).

##### 4.1 Theoretical Account via Drift-Diffusion Theory

To theoretically account for the new findings, we make some derivations that is partially similar to the ones in (Chun et al.,  
135 2005), but under a new constraint due to coagulations: "At contact ( $r = d$ ), radial component of the particle relative velocities

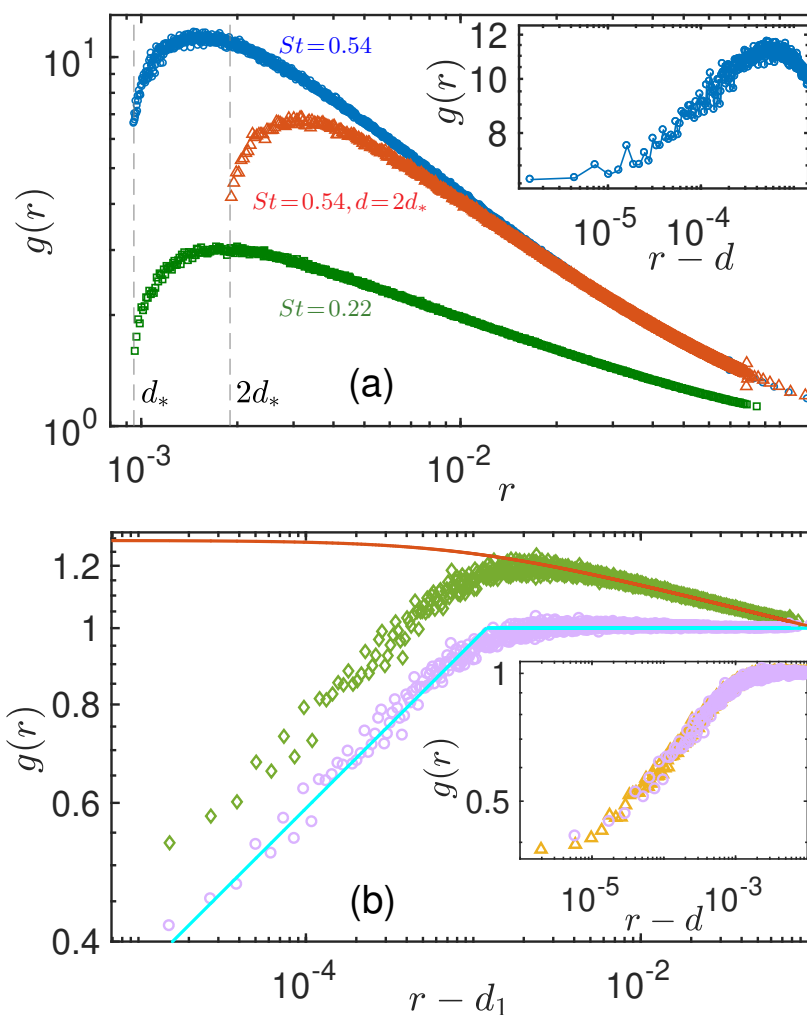


**Figure 1.** RDFs ( $g(r)$ ) of particles that coagulate upon collision. Note:  $d_* = 9.49 \times 10^{-4}$  (explanation in the text). **a)**  $g(r)$  for cases of different Stokes number and particle diameter ( $d$ ).  $\square$ :  $St=0.22$ ,  $d=d_*$ ,  $\circ$ :  $St=0.54$ ,  $d=d_*$ ,  $\triangle$ :  $St=0.54$ ,  $d=2d_*$ . All  $g(r)$  drop-off exponentially when  $r \rightarrow d$  (more details in text). **Inset:**  $g(r)$  versus  $r-d$  for the  $\circ$  case. It exemplify the fact that  $\lim_{r \rightarrow d} g(r)$  is nonzero. **b)** RDFs versus  $r-d_1$  (where  $d_1=0.99d$ ) for the case of  $St=0.054$ ,  $d=d_*$ .  $\diamond$ : the raw observed RDF. Red-line: power-law fit to the raw RDF (i.e. to the  $\diamond$ -plot) in the large- $r$  regime (the formula of the resultant curve is  $0.890r^{-0.0535}$ ). It is also the expected  $g(r)$  for non-colliding particles under the same conditions, thus it is equivalent to  $g_s(r)$  in the ansatz  $g_a(r) = g_0(r)g_s(r)$  (details in text).  $\circ$ : the compensated RDF, defined as the raw RDF divided by  $g_s(r)$  (note:  $g_s(r)$  is the RDF expected for non-colliding particles under the same condition), this may be understood as a ‘modulation’ on the RDF due to collision-coagulation and is expected to be  $St$ -independent, in the first-order. Cyan-line: two-piece power-law fits to the compensated-RDF (the  $\circ$ -plot) in the small and large  $r-d_1$  regimes respectively (fit results:  $4.17(r-d_1)^{0.212}$ ,  $1.00(r-d_1)^{-2 \times 10^{-4}}$ ), this is thus a 1st-order model of  $g_0(r)$ . **Inset:** RDFs versus  $r-d$ .  $\circ$ : compensated RDF for  $St=0.054$ ,  $d=d_*$ , equivalent to the  $\circ$ -plot in the panel’s main figure;  $\triangle$ :  $g(r)$  for the case of  $St=0.001$ ,  $d=d_*$ , i.e. particles with almost zero- $St$  but finite size. Comparison of the last two plots suggests that  $g_0(r)$  has negligible  $St$ -dependence.



can not be positive<sup>3</sup>, while with increasing  $r$  the constraint is gradually relaxed." The first consequence of this is that the distribution of the radial component of the relative particle velocity ( $W_r$ ) is highly asymmetric at  $r \approx d$ , i.e. the PDF of positive  $W_r$ 's are very small (this constitute the "enhanced asymmetry" mentioned earlier). Thus for  $r \approx d$ , the mean of  $W_r$ , i.e.  $\langle W_r \rangle$ , must be predominantly negative. From this, one could derive, in the limit of  $St \ll 1$ , a master equation (details in Sec. 3 or  
 140 (Chun et al., 2005)):

$$\frac{\partial \langle P \rangle}{\partial t} + \frac{\partial}{\partial r_i} (q_i^d + q_i^D) + \frac{\partial (\langle W_i \rangle \langle P \rangle)}{\partial r_i} = 0, \quad (5)$$

where  $P(\mathbf{r})$  is the PDF of finding another particle at position  $\mathbf{r}$  from a 'primary' particle<sup>4</sup>,  $\langle \cdot \rangle$  implies averaging over all primary particle trajectories (e.g.  $\langle W_r \rangle \equiv$  unconditional mean of  $w_r$ ),  $q_i^d$  is the drift flux (of probability due to turbulent fluctuation) and  $q_i^D$  the diffusive flux.

145 As described in Sec. 3, the definition of the drift flux is :  $q_i^d = - \int_{-\infty}^t \langle W_i(\mathbf{r}, t) \frac{\partial W_i}{\partial r_i'}(\mathbf{r}', t') \rangle \langle P \rangle(\mathbf{r}', t') dt'$ , and the diffusive flux is:  $q_i^D = - \int_{-\infty}^t \langle W_i(\mathbf{r}, t) W_j(\mathbf{r}', t') \rangle \frac{\partial \langle P \rangle}{\partial r_j'}(\mathbf{r}', t') dt'$ , where  $\mathbf{r}'$  satisfies a characteristic equation:  $\frac{\partial r_i'}{\partial t'} = W_i(\mathbf{r}', t')$ . We then expand  $W_i$ ,  $\frac{\partial W_i}{\partial r_i}$  and (consequently) the fluxes as perturbation series with  $St$  as the small parameter (details in (Supplements) or (Chun et al., 2005)). The coagulation constraint has nontrivial effects on the coefficients of these series. For the drift flux, the leading order terms (in powers of  $St$ ) are:

$$150 \quad q_i^d = - \langle P \rangle(\mathbf{r}) r_k \int_{-\infty}^t \left[ A_{ik}^{(1)} St + A_{ki}^{(2)} St^2 \right] dt', \quad (6)$$

with  $A_{ik}^{(1)} = \tau_\eta \langle \Gamma_{ik}(t) \Gamma_{lm}(t') \Gamma_{ml}(t') \rangle$  and  $A_{ki}^{(2)} = \tau_\eta^2 \langle \Gamma_{ij}(t) \Gamma_{jk}(t) \Gamma_{lm}(t') \Gamma_{ml}(t') \rangle$ ;  $\Gamma_{ij}$  is the  $ij$ -th component of the fluid's velocity gradient tensor at the particle position. As explained above, coagulation-constraint causes the PDF of relative particle velocities to become highly asymmetric for  $r \sim d$ , thus  $A_{ik}^{(1)}$  is nonzero at these scale. This is very different to the case of non-colliding particles (Chun et al., 2005) where  $A_{ik}^{(1)}$  is always zero due to statistical isotropy. We found that under the constraint,  
 155 DNS gives  $\int_{-\infty}^t A_{ik}^{(1)} dt' \approx -0.18$  and  $\int_{-\infty}^t A_{ki}^{(2)} dt' \approx 2.45$  (more in (Supplements)). Thus for  $r \sim d$ , the drift flux is negative for large  $St$  but becomes positive when  $St$  decreases below a value of order 0.01; and in the limit of  $St \rightarrow 0$ , it is dominated by the first term in (6).

$q_i^D$  is a 'nonlocal' diffusion caused by fluctuations and can be estimated using a model that assume the particle relative motions are due to a series of random straining flows (Chun et al., 2005). Chun et al. (2005) showed that, generally,  $q_i^D$  has  
 160 an integral form (due to nonlocality), and only in the special case where  $g(r)$  is a power-law, may it be cast into a differential form (similar to a local diffusion). In view of the nontrivial  $g(r)$  observed here, we must proceed with the integral form:

$$q_r^D = c_{st} r \int d\Omega \int_0^\infty dt_f F(t_f) \int_{d/r}^\infty dR_0 R_0^2 \langle P \rangle(rR_0) f_I(R_0, \mu, t_f),$$

where  $R_0 \equiv r_0/r$  with  $r_0$  as the initial separation distance of a particle pair before a straining event;  $F$  the probability density function for the duration of each event;  $f_I$  is determined by relative prevalence of extensional versus compressional strain

<sup>3</sup>In other words particles may approach each other (and collide) but they can not be created at contact and then separate.

<sup>4</sup>borrowing the notation of CK-theory (Chun et al., 2005),  $W_i, P$  are ensemble-averages over trajectories of satellite (secondary) particles around a primary particle whose history (including the fluid's velocity gradient tensor around it) is known and fixed.



165 events (more details in (Supplements) or (Chun et al., 2005)); note: due to coagulation, the  $R_0$ -integration starts from  $d/r$ . We differ crucially from the CK theory via the introduction of the factor  $c_{st}$ , which is positive, of order  $\lesssim 1$  and may depend on  $St$  (more in (Supplements)); .

By definition,  $g(r) \equiv \alpha \langle P \rangle$ . Periodic boundaries in our DNS imply that  $\alpha = V$ , (more in (Supplements)). Using this and the fact that the problem has only radial ( $r$ ) dependence, we rewrite (5) as:

$$170 \quad r^2 \frac{\partial g(r, t)}{\partial t} + \frac{\partial}{\partial r} [r^2 \alpha (q_i^d + q_i^D) + r^2 \langle W_r \rangle g(r, t)] = 0, \quad (7)$$

where the content inside  $[\cdot]$  gives the total flux. For a system in steady-state, the first term in (7) is zero, and upon integrating with limits  $[d, r]$ , we have:

$$175 \quad c_{st} r^3 \int_0^\infty d\Omega \int_0^\infty dt_f F(t_f) \int_{d/r}^\infty dR_0 R_0^2 g(r R_0) f_I(R_0, \mu, t_f) + g(r) [r^2 \langle W_r \rangle - Ar^3] = -R_c^*, \quad (8)$$

where we have identify the total flux at contact ( $r = d$ ) as the negative of the (always positive) normalized collision rate  $R_c^* \equiv R_c / (4\pi[N(N-1)/2]/V)$ , and comparing with (6), we see that:

$$A \equiv St \int_{-\infty}^t A_{ik}^{(1)} dt' + St^2 \int_{-\infty}^t A_{ki}^{(2)} dt', \quad (9)$$

180 with the specific values of the  $t'$ -integrals already given above. For clarity, one should note that on the left of Eq. (8), we have the diffusive flux ( $q_r^D$ ), the mean-field flux ( $r^2 g(r) \langle W_r \rangle$ ), the drift flux ( $q_r^d$ ); while on the right, the total flux is given in terms of the normalized collision rate ( $R_c^*$ ). We note that this equation contains the relationship among RDF, MRV and collision rate, besides other information.

## 4.2 Ansatz and Solution

Simple analytical solution to Eq. (8) may be elusive due to its integral nature (which follows from non-locality of the diffusive-  
 185 flux). However, one could gain insights into it and test its accuracy using numerical solutions. To do that, we begin with a simple ansatz for  $g(r)$  and show that (8) could numerically predict  $\langle W_r \rangle(r)$  with reasonable accuracy. The ansatz has the form  $g_a(r) = g_s(r)g_0(r)$ , with  $g_s(r) = c_0 r^{-c_1}$  i.e. the RDF for non-colliding particles (Chun et al., 2005). To keep things simple (as a first order analysis), we let  $g_0$  takes the simplest form that could still capture the main features of the RDFs as seen in Fig. 1, namely  $g_0(r) = c_{00}(r - d_1)^{c_{10}}$ . In words,  $g_0$  is a two-piece power-law of  $r - d_1$ , where  $c_{00}(r), c_{10}(r)$  are piece-wise  
 190 constants that switch from one fixed value to another at a crossover-scale  $r_c$  (of the order of  $d$ ). The values of  $c_{00}$  and  $c_{10}$  are determined from the DNS produced RDF, by fitting power-laws to the small and large  $r$  regimes ( $r_c$  results naturally from the intersection of the two power-law fits). The fact that we have found  $g(r \rightarrow d) > 0$  implies that  $d_1 < d$ ; also we shall see that  $d_1$  has negligible  $St$ -dependence when  $St$  is small. An example of the ansatz is shown Fig. 1b for the case of  $St = 0.05$  (the red-line is  $g_s$ , cyan-line is  $g_0$ ).



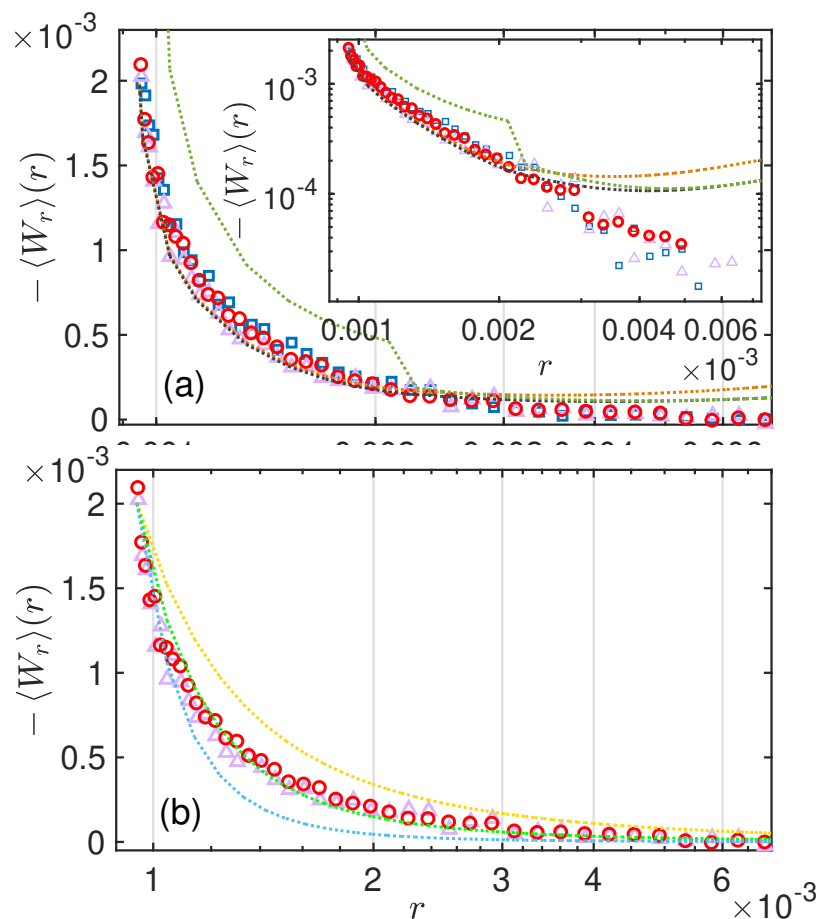


**Figure 2.** Mean radial component of relative velocity (MRV) for particles of specific Stokes numbers and some theoretic-numerical predictions. **a)** The markers are DNS results with  $\triangle$ :  $St=0.001$ ;  $\circ$ :  $St=0.054$ ;  $\square$ :  $St=0.11$ . The colored lines are the various numerical predictions using the theories (equation (8) or (12)) and the ansatz (details in text). Orange-line:  $\langle W_r \rangle_{r \sim d, St=0.054}$ , namely the numerical prediction using the integral version of the theory (Eq. (8)) for the small- $r$  regime (i.e.  $r \sim d$ ); black-line:  $\langle W_r \rangle_{r \gg d, St=0.054}$ , same as the previous but for the large- $r$  regime ( $r \gg d$ ); green-line: numerical predictions using the differential version of the theory (Eq. (12)). **Inset** A repeat of the main figure in log-log axes. **b)** MRV for particles compared with predictions based on phenomenological model of particle approach angles (Eq. (10) and (11)). The markers are DNS results with  $\triangle$ :  $St=0.001$ ;  $\circ$ :  $St=0.054$ . Dotted lines are model predictions of  $\langle W_r \rangle_{St=0}$  using (10) and (11) with variance  $K$  obtained by matching the model's and DNS's transverse to longitudinal ratio of structure functions (TLR) of a certain order. From the top, yellow-line: order 2, green-line: order 4, cyan-line: order 6.



195 Next, we numerically evaluate the first term in (8). As we are working in the small  $St$  limit, we approximate  $g(r, St)$  in this term using  $g(r, St \rightarrow 0)$  (a practice borrowed from (Chun et al., 2005)). Specifically, we replace  $g(r, St)$  with the ansatz fitted to the DNS data of  $g(r, St=0.001)$ . Using the DNS data, we then estimate  $A$ , compute  $R_c^*$  and  $c_{st}$  (it can be shown that  $c_{st} = |c_1|$  (more in (Supplements))). Finally we use (8) to predict  $\langle W_r \rangle(r)$ .

200 Comparison of the predicted  $\langle W_r \rangle(r)$  with the ones obtained directly from the DNS is shown in Fig. 2. As shown earlier, for  $r \sim d$ ,  $A$  is given by (9). However, as stated earlier, as  $r$  increases, the (statistical) asymmetry induced by collision-coagulation gradually become subdominant to the isotropy of turbulent-fluctuation. Statistical isotropy implies  $A_{ik}^{(1)} = 0$  (Chun et al., 2005), which our DNS confirms. Thus, for  $r \gg d$ ,  $A$  only depends on the order  $St^2$  term in (9), same as the finding in (Chun et al., 2005) for non-colliding particles. For this reason, we show two versions of the predicted  $\langle W_r \rangle$ , i.e.  $\langle W_r \rangle_{r \sim d}$  and  $\langle W_r \rangle_{r \gg d}$  which are obtained by setting  $A$  to its small- $r$  and large- $r$  limits ( $-2.6 \times 10^{-3}$ ,  $7.1 \times 10^{-3}$ ) respectively. The agreement between  
 205 the DNS and the predictions is remarkable, especially for small  $r$ . At  $r \approx 2d$ , the DNS result shows a weak tendency to first follow the upward trend of  $\langle W_r \rangle_{r \sim d}$  and then falls off significantly at  $r \gtrsim 2.5d$ , as implied by  $\langle W_r \rangle_{r \gg d}$ , albeit with a rate sharper than predicted.

### 4.3 Phenomenological Model of MRV

Alternatively, if MRV of fluid particles  $\langle W_r \rangle_{St=0}$  is known, one may assume that in the small  $St$  limit, particle velocity statistics are tied to their fluid counterparts (Chun et al., 2005), thus (8) may be used, with  $\langle W_r \rangle_{St=0}$ , to predict RDF (i.e.  $g(r, St)$ ). Fig. 2a shows that  $\langle W_r \rangle_{St>0}$  from the DNS do not change significantly for  $St \in [0.001, 0.1]$ , supporting this approach. Here we provide a simple, first order model for  $\langle W_r \rangle_{St=0}$ . We limit ourselves to the regime of small particles i.e.  $d \ll \eta$ ; and anticipate that  $\langle W_r \rangle$  is non-trivial (nonzero) only for  $r \sim d$ , a fact observable in Fig. 2a. We also assume that the relative trajectories of particles are rectilinear at such small scales. The coagulation constraint then implies that: in the rest frame of a particle (call  
 215 it P1), a second particle nearby must move in such a way that the angle ( $\theta$ ) between its relative velocity and relative position (seen by P1) must satisfies:  $\sin^{-1}(d/r) \leq \theta \leq \pi$ , under the convention of  $\sin^{-1}(x) \in [-\frac{\pi}{2}, \frac{\pi}{2}]$ , (more in (Supplements)). We can thus write (by treating negative and positive  $w_r$  separately, applying the K41-theory (Kolmogorov, 1941) and the bounds on  $\theta$ , details in (Supplements)), for  $St \ll 1$ , that:

$$220 \quad \langle W_r \rangle \equiv \langle w_r \rangle_* = p_- \langle w_r | w_r < 0 \rangle_* + p_+ \langle w_r | w_r \geq 0 \rangle_*$$

$$\approx -p_- \xi_- r + p_+ \xi_+ r \left[ 1 + \frac{\int_{\theta_m}^0 P_\theta^+(\theta') \cos(\theta') d\theta'}{\int_0^{\frac{\pi}{2}} P_\theta^+(\theta') \cos(\theta') d\theta'} \right], \quad (10)$$

where  $\langle \cdot \rangle_*$  denotes averaging over all particle pairs,  $p_+$  ( $p_-$ ) is the probability of a realization of  $w_r$  being positive (negative), and  $P_\theta^+$  is a conditional PDF such that  $P_\theta^+ \equiv P(\theta | w_r \geq 0) \equiv P(\theta | \theta \in [0, \frac{\pi}{2}])$ ,  $\theta_m$  is the minimum of  $\theta$  described above.  
 225 For a first order account, we neglect skewness in the distribution of particle relative velocities and set  $p_\pm = 0.5$ . Following (Kolmogorov, 1941), we have set  $\langle w_r | w_r < 0 \rangle_* = \xi_- r$ , where  $\xi_\pm = 0.76 \sqrt{\varepsilon / (15\nu)}$ , ('0.76' results from matching  $\xi_- r$  to the first-order fluid velocity structure-function seen in the DNS).



A simple phenomenological model for  $P(\theta)$  may be constructed using the (statistical) central-limit-theorem by assuming that the angle of approach  $\theta$  at any time is the sum of many random-incremental rotations in the past, thus we write:

$$230 \quad P(\theta) = N \exp[K \cos(\theta - \mu_\theta)] \sin(\theta), \quad (11)$$

where  $N \exp[\dots]$  is the circular normal distribution, i.e. analog of Gaussian distribution for angular data;  $\sin(\theta)$  results from integration over azimuthal angles ( $\phi$ ). We set  $\mu_\theta = \frac{\pi}{2}$  (neglect skewness in fluid's relative velocity PDF) and obtain  $K$  by matching the transverse to longitudinal ratio of structure functions (TLR) of the particle relative velocities with the ones via the DNS data;  $N$  is determined via normalization of  $P(\theta)$ . Fig. 2b shows the  $\langle w_r \rangle_*$  derived via (10) and (11), using  $K$  calibrated  
 235 with TLR of 2nd, 4th, 6th order structure functions respectively. The results have correct qualitative trend of vanishing values at large  $r$  that increases sharply as  $r$  approach  $d$ , with the 4th-order's result giving the best agreement with DNS. Currently we have not a satisfactory rationale to single out the 4th-order. The TLR of different orders give differing results may imply that our first-order model may be incomplete, possibly due to over-simplification in (11) or to the inaccuracy of the rectilinear assumption ( $d/\eta$  in the DNS may be insufficiently small).

#### 240 4.4 Differential Version of the Theory and Its Validity

We now discuss an important but precarious theoretical issue. Chun et al. (2005) clearly showed that the non-local diffusion ( $q_r^D$ ) may be converted, from its general integral form, into a differential version only when the underlying RDF is a simple power-law. However, Lu et al. (2010) and Yavuz et al. (2018), working in two very different scenarios, found that their predictions using the differential form of the theory agree well with experiments, even when the RDFs involved was clearly not  
 245 power-laws. We shall attempt to remedy this apparent paradox in future work. To examine how well this albeit unjustified method works here, we recast (8) into its differential form (Chun et al., 2005):

$$-\tau_\eta^{-1} B_{nl} r^4 \frac{\partial g}{\partial r} + g(r) [r^2 \langle W_r \rangle - Ar^3] = -R_c^*, \quad (12)$$

where  $B_{nl} = 0.0397$  (this value is computed from our DNS,  $B_{nl}$  is expected to depend on flow characteristics e.g.  $R_\lambda$  and  $\tau_\eta$  (more in (Supplements))). Using (12), the same  $g_s g_0$  ansatz and  $A = 7.1 \times 10^{-3}$ , we make another prediction for  $\langle W_r \rangle$ , which  
 250 is plotted in Fig. 2a (green dash-line). The accuracy of the new prediction is worse (the jump correspond to the kink in the ansatz) but still on par with results above.

One advantage of (12) is that it admits of a general solution, which we now give, assuming  $\langle w_r \rangle_*$  is given by (10) & (11):

$$g(r) = \frac{1}{\beta(r)} \left[ \int \beta(r) q(r) dr + C \right], \quad (13)$$

with  $q(r) = R_c^* \tau_\eta / (B_{nl} r^4)$ ;  $\beta(r) = \exp \left[ \int p(r) dr \right]$ ;  $p(r) = [Ar - \langle w_r \rangle_*] \tau_\eta / (B_{nl} r^2)$ , (more in (Supplements)).

## 255 5 Conclusions

To conclude, we observed that collision strongly affects the RDF and MRV and imposes strong coupling between them. This challenges the efficacy of a "separation paradigm" and suggests that results from any studies that preclude particle collision has



limited relevance for predicting collision statistics<sup>5</sup>. We have presented a theory for particle collision-coagulation in turbulence (based on a Fokker-Planck framework) that explains the above observations and verified its accuracy by showing that  $\langle W_r \rangle$  could be accurately predicted using a sufficiently accurate RDF. The theory account for the full collision-coagulation rate which include contributions from mean-field and fluctuations; and as such, our work complements and completes earlier mean-field theories (Saffman and Turner, 1956; Sundaram and Collins, 1997). We showed that a simple model of particle approach-angles could capture the main features of  $\langle W_r \rangle$ . We uncovered the unexplained accuracy of the differential drift-diffusion equation (see discussion around (12)). Our findings provide a new understanding of particle collision and its relation with clustering and relative motion, which has implications for atmospheric clouds or generally to systems involving colliding particles in unsteady flows.

*Author contributions.* All the authors made significant contributions to this work.

*Competing interests.* The authors declare no competing financial interests.

*Acknowledgements.* This work was supported by the National Natural Science Foundation of China (Grant 11872382) and by the Thousand Young Talent Program of China. We thank Jialei Song for helps. We thank Wai Chi Cheng, Jianhua Lv, Liubin Pan, Raymond A. Shaw for discussion and suggestions.

---

<sup>5</sup>The current statement also holds for other types of collisional outcomes (not only for collision-coagulation), but the specific outcomes should be qualitatively different from the current case.



## References

- Arfken, G. B. and Weber, H. J.: *Mathematical methods for physicists*, 1999.
- Balkovsky, E., Falkovich, G., and Fouxon, A.: Intermittent Distribution of Inertial Particles in Turbulent Flows, *Phy. Rev. Lett.*, 86, 2790, 275 2001.
- Bec, J., Biferale, L., Cencini, M., Lanotte, A., Musacchio, S., and Toschi, F.: Heavy Particle Concentration in Turbulence at Dissipative and Inertial Scales, *Phy. Rev. Lett.*, 98, 084 502, 2007.
- Chun, J., Koch, D. L., Rani, S. L., Ahluwalia, A., and Collins, L. R.: Clustering of aerosol particles in isotropic turbulence, *J. Fluid Mech.*, 536, 219–251, 2005.
- 280 Dou, Z., Bragg, A. D., Hammond, A. L., Liang, Z., Collins, L. R., and Meng, H.: Effects of Reynolds number and Stokes number on particle-pair relative velocity in isotropic turbulence: a systematic experimental study, *Journal of Fluid Mechanics*, 839, 271–292, 2018.
- Falkovich, G., Fouxon, A., and Stepanov, M. G.: Acceleration of rain initiation by cloud turbulence, *Nature*, 419, 151, 2002.
- Grabowski, W. W. and Wang, L.-P.: Growth of cloud droplets in a turbulent environment, *Annual review of fluid mechanics*, 45, 293–324, 2013.
- 285 Ireland, P. J., Vaithianathan, T., Sukheswalla, P. S., Ray, B., and Collins, L. R.: Highly parallel particle-laden flow solver for turbulence research, *Computers & Fluids*, 76, 170–177, 2013.
- Johansen, A., Oishi, J. S., Mac Low, M.-M., Klahr, H., Henning, T., and Youdin, A.: Rapid planetesimal formation in turbulent circumstellar disks, *Nature*, 448, 1022–1025, 2007.
- Karnik, A. U. and Shrimpton, J. S.: Mitigation of preferential concentration of small inertial particles in stationary isotropic turbulence using electrical and gravitational body forces, *Physics of Fluids*, 24, 073 301, 2012.
- 290 Karpińska, K., Bodenschatz, J. F. E., Malinowski, S. P., Nowak, J. L., Risius, S., Schmeissner, T., Shaw, R. A., Siebert, H., Xi, H., Xu, H., and Bodenschatz, E.: Turbulence-induced cloud voids: observation and interpretation, *Atmospheric Chemistry and Physics*, 19, 4991–5003, <https://doi.org/10.5194/acp-19-4991-2019>, 2019.
- Kolmogorov, A. N.: The local structure of turbulence in incompressible viscous fluid for very large Reynolds numbers, *Dokl. Akad. Nauk SSSR*, 30, 299–303, 1941.
- 295 Lu, J., Nordsiek, H., Saw, E. W., and Shaw, R. A.: Clustering of Charged Inertial Particles in Turbulence, *Phys. Rev. Lett.*, 104, 184 505, 2010.
- Mortensen, M. and Langtangen, H. P.: High performance Python for direct numerical simulations of turbulent flows, *Computer Physics Communications*, 203, 53–65, 2016.
- 300 Onishi, R. and Seifert, A.: Reynolds-number dependence of turbulence enhancement on collision growth, *Atmospheric Chemistry and Physics*, 16, 12 441–12 455, <https://doi.org/10.5194/acp-16-12441-2016>, 2016.
- Pope, S. B.: *Turbulent Flows*, Cambridge Univ. Press, Cambridge, UK, 2000.
- Reade, W. C. and Collins, L. R.: Effect of preferential concentration on turbulent collision rates, *Phys. Fluids*, 12, 2530, 2000.
- Rogallo, R. S.: *Numerical experiments in homogeneous turbulence*, vol. 81315, National Aeronautics and Space Administration, 1981.
- 305 Saffman, P. and Turner, J.: On the collision of drops in turbulent clouds, *Journal of Fluid Mechanics*, 1, 16–30, 1956.
- Salazar, J. P. L. C., de Jong, J., Cao, L., S. H. Woodward, H. M., and Collins, L. R.: Experimental and numerical investigation of inertial particle clustering in isotropic turbulence, *J. Fluid Mech.*, 600, 245–256, 2008.



- Saw, E. W., Shaw, R. A., Ayyalasomayajula, S., Chuang, P. Y., and Gylfason, A.: Inertial Clustering of Particles in High-Reynolds-Number Turbulence, *Phys. Rev. Lett.*, 100, 214 501, 2008.
- 310 Saw, E.-W., Salazar, J. P., Collins, L. R., and Shaw, R. A.: Spatial clustering of polydisperse inertial particles in turbulence: I. Comparing simulation with theory, *New Journal of Physics*, 14, 105 030, 2012a.
- Saw, E.-W., Shaw, R. A., Salazar, J. P., and Collins, L. R.: Spatial clustering of polydisperse inertial particles in turbulence: II. Comparing simulation with experiment, *New Journal of Physics*, 14, 105 031, 2012b.
- Saw, E.-W., Bewley, G. P., Bodenschatz, E., Sankar Ray, S., and Bec, J.: Extreme fluctuations of the relative velocities between droplets in  
315 turbulent airflow, *Physics of Fluids*, 26, 111 702, 2014.
- Sundaram, S. and Collins, L.: Collision statistics in an isotropic particle-laden turbulent suspension. Part I. Direct numerical simulations, *J. Fluid Mech.*, 335, 75–109, 1997.
- Supplements: See Supplementry Material at... For ArXiv version, it is attached as appendix.
- Voßkuhle, M., Lévêque, E., Wilkinson, M., and Pumir, A.: Multiple collisions in turbulent flows, *Physical Review E*, 88, 063 008, 2013.
- 320 Wang, L.-P., Ayala, O., Rosa, B., and Grabowski, W. W.: Turbulent collision efficiency of heavy particles relevant to cloud droplets, *New Journal of Physics*, 10, 075 013, <https://doi.org/10.1088/1367-2630/10/7/075013>, 2008.
- Wilkinson, M., Mehlig, B., and Bezuglyy, V.: Caustic activation of rain showers, *Phys. Rev. Lett.*, 97, 48 501, 2006.
- Wood, A. M., Hwang, W., and Eaton, J. K.: Preferential concentration of particles in homogeneous and isotropic turbulence, *Int. J. Multiphase Flow*, 31, 1220, 2005.
- 325 Yavuz, M., Kunnen, R., Van Heijst, G., and Clercx, H.: Extreme small-scale clustering of droplets in turbulence driven by hydrodynamic interactions, *Phys. Rev. Lett.*, 120, 244 504, 2018.
- Zaichik, L. I. and Alipchenkov, V. M.: Pair dispersion and preferential concentration of particles in isotropic turbulence, *Phys. of Fluids*, 15, 1776, 2003.